

Synthesis of Monolithic Al₂O₃ with Well-Defined Macropores and Mesostructured Skeletons via the Sol–Gel Process Accompanied by Phase Separation

Yasuaki Tokudome,[†] Koji Fujita,^{*,†,‡} Kazuki Nakanishi,[§] Kiyotaka Miura,[†] and Kazuyuki Hirao[†]

Department of Material Chemistry, Graduate School of Engineering, Kyoto University, Katsura, Nishikyo-ku, Kyoto 615-8510, Japan, PRESTO, Japan Science and Technology Agency (JST), 4-1-8 Honcho Kawaguchi, Saitama, Japan, and Department of Chemistry, Graduate School of Science, Kyoto University, Kitashirakawa, Sakyo-ku, Kyoto 606-8502, Japan

Received December 22, 2006. Revised Manuscript Received April 26, 2007

Alumina (Al₂O₃) monoliths with well-defined macropores and mesostructured skeletons have been synthesized via a spontaneous route from the aqueous and ethanolic solution of aluminum salts in the presence of propylene oxide and poly(ethylene oxide) (PEO). The addition of propylene oxide to the starting solution controls the gelation, whereas the addition of PEO induces the phase separation. Appropriate choice of the starting composition, by which the phase separation and gelation concur, allows the production of bicontinuous macroporous Al₂O₃ monoliths in large dimensions (10 × 10 × 10 mm³). The size of macropores is controlled in the range of 400 nm to 1.8 μm, depending on the PEO content in starting solutions. The dried gel is amorphous, whereas heating at temperatures above 800 °C leads to the formation of crystalline phases without spoiling the macroporous morphology; nanocrystalline γ-Al₂O₃ is precipitated at 800 °C, α-Al₂O₃ starts to form at 1000 °C, and complete transformation into α-Al₂O₃ is achieved at 1100 °C for 5 h. Nitrogen adsorption–desorption measurements revealed that the skeletons of dried gels possess the mesostructure with a median pore size of about 2.6 nm and a surface area as high as 396 m²/g. Heat treatment at 300 °C increases the pore size and surface area to 3.5 nm and 512 m²/g, respectively. Even after heat treatment at 800 °C, which results in the formation of nanocrystalline γ-Al₂O₃, the surface area is 182 m²/g, with the pore size being 4.5 nm.

Introduction

Porous alumina (Al₂O₃) has attracted considerable attention because of its potential applications in various fields such as catalysis, adsorption, and separation.^{1,2} For these applications, many attempts have been carried out to fabricate Al₂O₃ that have structurally controlled pores on the length scale from the nanometer to the micrometer. For example, mesoporous Al₂O₃ can be prepared using self-organized arrays of long-chain surfactants or amphiphilic block copolymers as the templates.^{3–5} Latex-sphere templating extends the pore size up to the micrometer range.⁶ Another approach is anodic oxidation of aluminum,⁷ in which cylindrical uniformly sized nanoholes are hexagonally arranged in high regularity.

Hierarchically porous materials, e.g., macroporous materials with mesotexture, are highly desirable, especially in applications that utilize liquid-phase reactions, such as catalyst supports and separations. This is because the interconnected macroporous channels facilitate transport of the materials into mesopores where reactions can take place. A surfactant-assisted synthesis route produces Al₂O₃ with a bimodal pore size distribution;^{8,9} however, the integration of dual porous structures into large-dimension monoliths is still difficult to achieve; most hierarchically porous Al₂O₃ is dried to powders or highly cracked and fragile monoliths. This limits their utility in areas where processing or application dictates some structural form with moderate mechanical strength.

An exception is sol–gel-derived porous silica (SiO₂), which can be dried to monoliths without cracking and can be handled without damage. The controls over the materials shape broaden the applicability of SiO₂-based porous materials in the aforementioned diverse fields. A sol–gel method accompanied by phase separation has been well-established as a technique to fabricate SiO₂ monoliths with a bimodal pore structure from silicon alkoxide.¹⁰ In this approach, the phase separation and sol–gel transition concur by the

* To whom correspondence should be addressed: E-mail: fujita@dipole7.kuic.kyoto-u.ac.jp. Tel: 81-75-383-2432. Fax: 81-75-383-2420.

[†] Graduate School of Engineering, Kyoto University.

[‡] PRESTO, Japan Science and Technology Agency.

[§] Graduate School of Science, Kyoto University.

- (1) Downing, J. C.; Goodboy, K. P. *Claus Catalysis and Alumina Catalyst Materials and Their Application*; American Chemical Society: Washington, DC, 1990.
- (2) Schüth, F.; Sing, K. S. W.; Weitkamp, J. *Handbook of Porous Solids*; Wiley: New York, 2002.
- (3) Yada, M.; Machida, M.; Kijima, T. *Chem. Commun.* **1996**, 769.
- (4) Vaudary, F.; Khodabandeh, S.; Davis, M. *Chem. Mater.* **1996**, 8, 1451.
- (5) Bagshaw, S. A.; Pinnavaia, T. J. *Angew. Chem., Int. Ed.* **1996**, 35, 1102.
- (6) Holland, B. T.; Blanford, C. F.; Stein, A. *Science* **1998**, 281, 538.
- (7) Masuda, H.; Fukuda, K. *Science* **1995**, 268, 1466.

(8) Deng, B. W.; Toepke, M. W.; Shanks, B. H. *Adv. Funct. Mater.* **2003**, 13 (1), 61.

(9) Ren, T. Z.; Yuan, Z. Y.; Su, B. L. *Langmuir*, **2004**, 20, 1531.

(10) Nakanishi, K. *J. Porous Mater.* **1997**, 4, 67.

polymerization reaction to produce a wet gel with a bicontinuous structure, in which both gel-rich and solvent-rich phases are interconnected on the length scale of micrometer. After tailoring the micrometer-range structure, solvent exchange with a basic aqueous solution and subsequent heat treatment yield mesopores with diameters of 5–10 nm via Ostwald ripening,¹¹ leading to hierarchical dual pores throughout a monolithic gel. The SiO₂ monoliths with well-defined macropores and mesostructured skeletons exhibit some remarkable properties as the stationary phase of high-performance liquid chromatography (HPLC), compared to the conventional particle-packed systems.¹²

Because the preparation of macroporous monoliths via the sol–gel route accompanied by phase separation requires a relatively high concentration of alkoxide precursors, the reactivity of precursors significantly affects the feasibility of producing uniform, crack-free monoliths. The successful preparation of SiO₂ monoliths is primarily due to the ease of controlling the hydrolysis and polycondensation of silicon alkoxides. In contrast, aluminum alkoxides such as aluminum tri-isopropoxide or aluminum tri-*sec*-butoxide are highly reactive, and thus, the structural development during the hydrolysis and polycondensation is usually hard to control because of the rapid polymerization; in fact, so far, there have been no reports of macroporous Al₂O₃ monoliths using the sol–gel method accompanied by phase separation. A common strategy to tackle this problem is to reduce the reactivity of precursors either by using a strong acid or by the addition of chelating agents such as ethylacetoacetone;^{13,14} however, the challenge remains as to how to induce the homogeneous gelation throughout the solution. Another simpler but more straightforward route is desirable to fabricate the porous Al₂O₃ monoliths in a reproducible fashion.

Gash and co-workers^{15,16} have recently developed alkoxide-free, sol–gel techniques for the synthesis of robust, monolithic aerogels of various metal oxides including Al₂O₃. The aerogels were prepared by the addition of epoxides to aqueous and/or etanolic solutions of metal salts followed by drying under supercritical conditions. The epoxides work as an acid scavenger to raise the solution pH gradually, which drives the hydrolysis and condensation of hydrated metal species. The slow and uniform increase in the solution pH allows the homogeneous gelation to produce a monolithic gel. This technique would be very useful for designing macroporous monoliths or hierarchical macro–mesoporous monoliths as well as aerogels.

Table 1. Starting Compositions of Samples (in grams)

sample	AlCl ₃ ·6H ₂ O	PEO	EtOH	H ₂ O	propylene oxide
HP	4.32	0.04–0.12	4.35	4.00	3.11
MTP	4.32	0.12	2.37	7.00	3.11

In this paper, we demonstrate the preparation of hierarchical macro–mesoporous Al₂O₃ by combining the phase separation with the reliable and reproducible sol–gel route that allows the fabrication of robust, large-dimension Al₂O₃ monoliths from the solution of aluminum salts in the presence of propylene oxide. The resultant Al₂O₃ monoliths possess precisely controllable macropores and the mesostructured skeletons that yield a high surface area. To the best of our knowledge, this is the first report of the synthesis and characterization of such macro–mesoporous Al₂O₃ monoliths. A lot of benefits are expected to arise from the dual pore structure integrated in monoliths.

Experimental Section

Synthesis. The starting compositions of Al₂O₃ gels prepared in this study are listed in Table 1. AlCl₃·6H₂O (Aldrich, 99%) was used as an aluminum source, and a mixture of distilled H₂O and ethanol (EtOH) (Kishida Reagents Chemicals, 99.5%) as the solvent. Propylene oxide (Aldrich, ≥99%) was added to initiate gelation, and poly(ethylene oxide) (PEO) (Aldrich) having viscosity-averaged molecular weight (*M_v*) of 1 × 10⁶ was used as a polymer to induce the phase separation. All reagents were used as received. The content of PEO (in grams) will hereafter be often denoted as *w*_{PEO}.

We prepared gels from two systems, denoted as HP and MTP. A difference between HP and MTP is the volume ratio of H₂O to EtOH; the H₂O/EtOH ratio is larger for the MTP system than for the HP. The detail of gel preparation is as follows. First, AlCl₃·6H₂O and PEO were dissolved in a mixture of H₂O and EtOH. Propylene oxide was then added to the transparent solution under ambient conditions (25 °C). After stirring for 1 min, the resultant homogeneous solution was transferred into a glass tube. The tube was sealed and kept at 40 °C for gelation. After gelation, the wet gel was aged for 24 h and evaporation-dried at 40 °C. Some of the dried gels were heat-treated at various temperatures between 700 and 1100 °C for 5 h in air.

Characterization. Morphology of dried and heated gels was observed by a scanning electron microscope (SEM; S-2600N, Hitachi Ltd., Japan, Au coating). The size distribution of macropores was measured by a mercury porosimetry (Poresizer9320, Micromeritics Co., USA). Micro–mesoporous structure was characterized by a nitrogen adsorption–desorption isotherm (Tristar 3000, Micromeritics Co., USA). The pore size distribution was calculated from the adsorption branch of the isotherm by the Barrett–Joyner–Halenda (BJH) method, and the surface area was obtained by the Brunauer–Emmett–Teller (BET) method. For the purpose of clarifying the phase-separation behavior of the solution, we also carried out thermogravimetry (TG) and differential thermal analysis (DTA) with a Thermo plus TG 8120 instrument (Rigaku Co., Japan). The measurements were performed at a heating rate of 10 °C min^{−1} in air. X-ray diffraction (XRD) analysis with Cu Kα radiation (*λ* = 0.154 nm; RINT2500, Rigaku, Japan) was performed in order to identify the crystalline phases if precipitated. The measurements were carried out for the powder specimens prepared by grinding macroporous monoliths.

- (11) Iler, R.K. *The Chemistry of Silica, Solubility, Polymerization, Colloids and Surface Properties, and Biochemistry*; Wiley-Interscience: New York, 1979.
- (12) Minakuchi, H.; Nakanishi, K.; Soga, N.; Ishizuka, N.; Tanaka, N. *Anal. Chem.* **1996**, *68*, 3498; Tanaka, N.; Kobayashi, H.; Nakanishi, K.; Minakuchi, H.; Ishizuka, N. *Anal. Chem.* **2001**, *73*, 420A.
- (13) Sanchez, C.; Livage, J.; Henry, M.; Babonneau, F. *J. Non-Cryst. Solids* **1988**, *100*, 65.
- (14) Tadanaga, K.; Iwami, T.; Tohge, N.; Minami, T. *J. Sol–Gel Sci. Technol.* **1994**, *3*, 5.
- (15) Gash, A. E.; Tillotson, T. M.; Satcher, J. H., Jr.; Poco, J. F.; Hrubesh, L. W.; Simpson, R. L. *Chem. Mater.* **2001**, *13*, 999.
- (16) Baumann, T. F.; Gash, A. E.; Chinn, S. C.; Sawvel, A. M.; Mawell, R. S.; Satcher, J. H., Jr. *Chem. Mater.* **2005**, *17*, 395.

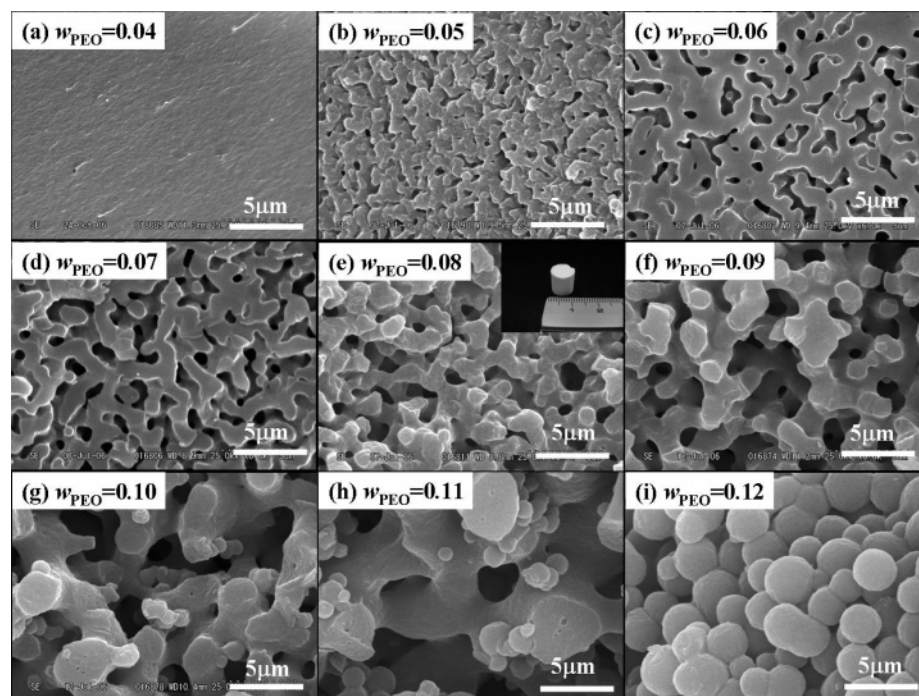


Figure 1. SEM photographs of dried Al₂O₃ gels prepared from the HP system with varied PEO content: w_{PEO} = (a) 0.04, (b) 0.05, (c) 0.06, (d) 0.07, (e) 0.08, (f) 0.09, (g) 0.10, (h) 0.11, and (i) 0.12.

Results and Discussion

The starting solutions prepared from the compositions listed in Table 1 were initially homogeneous and transparent. As time elapsed, the phase separation and the gelation proceeded spontaneously in a closed and static condition at a constant temperature (40 °C). The gels prepared from the solution containing propylene oxide formed quite quickly (~10 min), although gelation did not take place in the solution without propylene oxide. As Gash and co-workers¹⁶ have previously shown, gelation of metal salts solution is induced by using epoxides as gelation initiators. Epoxides act as an irreversible proton scavenger and cause the solution pH to increase gradually throughout the solution.¹⁵ In the present HP synthesis, the solution pH was <1 before the addition of propylene oxide, increased gradually with time, and reached 3 immediately before the gelation, i.e., at about 10 min. The slow and uniform pH rise drives the hydrolysis and condensation of the hydrated metal cations to form the monolithic gel. On the other hand, the addition of PEO to the starting solution did not have such a deep impact on the gelation time but induced the formation of phase-separating structures. For the HP system, the appearance of the resultant gels depended on the PEO content in the starting composition. When the PEO content was small, colorless and transparent or white and translucent gels were obtained. As the PEO content was increased, the gels became opaque. As for the MTP system, the gel with high density settled down because of the gravity effect and macroscopically exhibited two phases, i.e., precipitated and supernatant phases.

Figure 1 shows the SEM images of dried gels prepared from the HP system with varied PEO contents. The gel morphology depends significantly on the PEO content. As the PEO content is increased, the gel morphology in the micrometer range changes from nonporous (Figure 1a),

through bicontinuous structure (Figure 1b–g), to particle aggregates (Figure 1i). The gel morphology is determined by the timing of the onset of phase separation relative to the gelation. The phase separation tendency is related to the miscibility of a polymeric system, which can be estimated by the Flory–Huggins formulation.^{17–19} The Gibbs free energy change of mixing, ΔG , can be described as follows

$$\Delta G \propto RT \left(\frac{\phi_1}{P_1} \ln \phi_1 + \frac{\phi_2}{P_2} \ln \phi_2 + \chi \phi_1 \phi_2 \right) \quad (1)$$

where χ is the interaction parameter, ϕ_i and P_i are the volume fraction and the degree of polymerization of component i ($i = 1$ or 2), respectively, R is the gas constant, and T is the temperature. The former two terms in parenthesis represent the entropic contribution, and the last term the enthalpic contribution. In the SiO₂ sol–gel system in the presence of poly(acrylic acid), the phase separation is driven by the entropy loss due to the polymerization of SiO₂ oligomers, whereas the enthalpy-driven phase separation is observed for the SiO₂ systems in the presence of PEO, where there exists a repulsive interaction between solvent mixture and PEO adsorbed on alkoxy-derived oligomers through hydrogen bonds.¹⁰ As mentioned below, entropy loss contributes essentially to ΔG in the present system, which causes the phase separation. Namely, P_1 in eq 1 becomes large as a result of the homogeneous condensation reaction of Al₂O₃ oligomers due to the uniform increase in solution pH, which makes ΔG larger. Thus, the system phase-separates during the condensation of hydrated aluminum species. When phase separation occurs much later than gelation, transparent gels

(17) Flory, P. J. *J. Chem. Phys.* **1942**, *10*, 51.

(18) Huggins, M. J. *Phys. Chem.* **1942**, *46*, 151.

(19) Huggins, M. J. *Am. Chem. Soc.* **1942**, *64*, 1712.

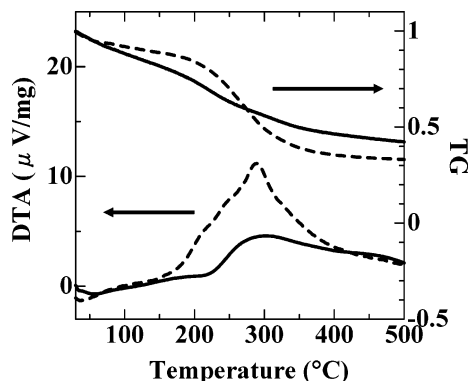


Figure 2. TG-DTA curves of precipitated phase (solid lines) and supernatant phase (dash lines) obtained from the MTP system.

with nanometer-sized pores, i.e., nonporous gels in the micrometer range, can be obtained as monoliths (see Figure 1a). On the contrary, when phase separation takes place much earlier than gelation, the bicontinuous structure fragments into spherical particles to reduce the interfacial energy (Figure 1i). Nearly concurrent sol–gel transition and phase separation produce the bicontinuous monolithic structure (Figure 1b–h), in which each of the gel phase and the fluid phase is three-dimensionally interconnected on the length scale of micrometers. After evaporation drying, the fluid phase composed mainly of solvent mixture turns into continuous macropores, and the gel phase becomes skeletons. From the inset of Figure 1e, one can see the formation of monolithic circular cylinder of Al_2O_3 gel in large dimensions (the diameter of top and bottom faces is ~ 10 mm, the height is ~ 10 mm). Close looks at images g and h of Figure 1 reveal the existence of small particles in the continuous macroporous network. This kind of morphology is observed as a result of the secondary phase separation of the fluid phase.¹⁰

To clarify the role for PEO in phase separation, we carried out thermal analysis so that the distribution of PEO between the gel and fluid phases during the phase separation could be deduced. Measurements were performed for the precipitate and supernatant phases derived from the MTP system in which the gelation time was prolonged by the increased $\text{H}_2\text{O}/\text{EtOH}$ volume ratio, and hence, the morphology of macroscopically two phases was obtained because of too early onset of phase separation relative to gelation. TG and DTA curves for the precipitate and supernatant phases are shown in Figure 2. The evaporation of residual solvent components takes place at temperatures below 100 °C for both the precipitate and supernatant phases. The exothermic peak at around 300 °C as observed for the precipitated phase is attributed to the pyrolysis of organic species, such as halogenated alcohol, generated by the ring-opening reaction of protonated propylene oxide, because the peak is detected even in the gels prepared in PEO-free conditions (not shown). The decomposition of PEO is observed only for the supernatant phase as a pronounced weight loss between 200 and 300 °C accompanied by the large exothermic peak. This result indicates that PEO is preferentially distributed into the fluid phase composed mainly of solvent mixtures, which suggests that the interaction between polymerizing alumina oligomers and PEO is less attractive. This situation is quite different from those observed in PEO-incorporated alkoxy-derived

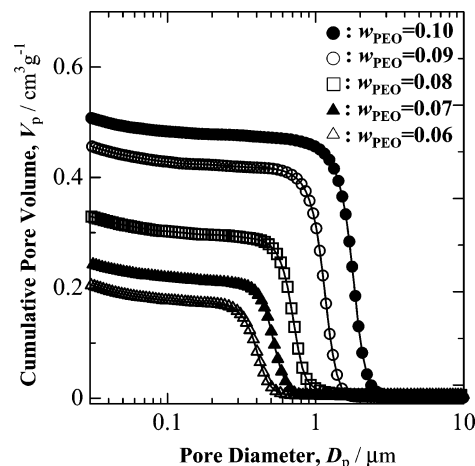


Figure 3. Pore size distributions of dried Al_2O_3 gels prepared from the HP system with $w_{\text{PEO}} = (\Delta)$ 0.06, (\blacktriangle) 0.07, (\square) 0.08, (\circ) 0.09, and (\bullet) 0.10.

SiO_2 sol–gel systems, where PEO is preferentially distributed into the precipitate phase when the morphology of macroscopic two phases is obtained.¹⁰ The driving force for the phase separation in the SiO_2 sol–gel systems in the presence of PEO is ascribed to the hydrophobic–hydrophilic repulsive interaction between solvent mixtures and PEO adsorbed on alkoxy-derived oligomers (enthalpic contribution). In the present system where the interaction between polymerizing oligomers and PEO is very weak, however, the phase separation is dominated by the entropic contribution rather than enthalpic one. Namely, the increase in the degree of polymerization, i.e., the large value of P_1 in eq 1, brings about the reduction of compatibility between polymerizing Al_2O_3 oligomers and PEO chain, which leads to the phase separation.

Figure 3 shows the pore size distributions measured for bicontinuous macroporous Al_2O_3 gels using mercury porosimetry. Each of the dried gels possesses a sharp pore size distribution, which implies that the phase-separated structure is formed via spinodal decomposition as proven in the preceding studies.¹⁰ The increase in pore size with an increase in PEO content is ascribed to the increased phase-separation tendency, because spinodal decomposition involves a coarsening process in the course of the formation of phase-separated structures.¹⁰ In the present systems, the increase in PEO content reduces the compatibility between polymerizing Al_2O_3 oligomers and PEO significantly, and thus, the onset of phase separation relative to gelation is accelerated to produce the coarsened bicontinuous structure, with the larger macropores being left behind after drying. It is found from Figure 3 that the pore size is controlled between 400 nm to 1.8 μm . On the other hand, the pore volume is mainly determined by the PEO content because PEO is distributed in the fluid phase that turns into the macropores after drying. Hence, the pore volume also increases with increasing PEO content. The shrinkage of gels during the drying process may contribute partly to the variation of pore volume, because the gels prepared with lower PEO content exhibit the larger degree of shrinkage.

Variation of XRD pattern with heat-treatment temperature is depicted in Figure 4. The measurements were performed

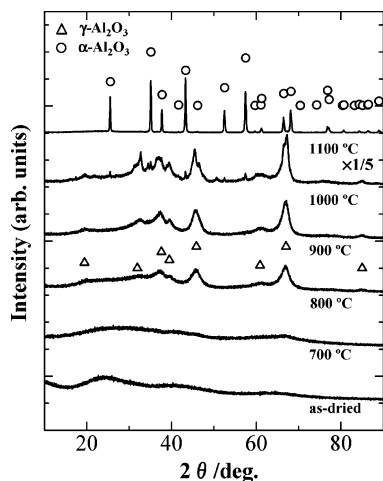


Figure 4. Variation of XRD pattern with heat-treatment temperature. The measurements were carried out for the samples prepared from the HP system with $w_{\text{PEO}} = 0.09$. Symbols Δ and \circ represent the diffraction peaks ascribed to γ -Al₂O₃ and α -Al₂O₃ phases, respectively.

for the samples prepared from the HP system with $w_{\text{PEO}} = 0.09$. No discernible peaks are found for the dried gel, indicating the amorphous structure. Crystalline phases such as boehmite (AlOOH) or pseudo-boehmite (less-well-crystallized boehmite, or gelatinous boehmite) were often observed in the aerogels or xerogels derived from aluminum alkoxides or salts.^{20–22} The degree of crystallinity is affected by several factors, including precursor concentration, reaction pH, the amount and kind of solvents, temperature, and the presence or absence of polymers in the starting solution. The formation of amorphous Al₂O₃ gels in the present case is presumably related to the gelation under the acid condition using a high concentration of aluminum salts. The sample remains amorphous even after the heat treatment at 700 °C, whereas the diffraction peaks ascribed to γ -Al₂O₃ appear upon heating at 800 and 900 °C. The width of diffraction peaks is broad, indicating the precipitation of nanocrystalline γ -Al₂O₃ from the amorphous phase. The crystallite size estimated by Scherrer's equation is approximately 3.9 and 5.2 nm for the samples heat-treated at 800 and 900 °C, respectively. When the heat-treatment temperature is higher than 1000 °C, γ -Al₂O₃ phase diminishes gradually, and instead, α -Al₂O₃ phase appears. A single phase of α -Al₂O₃ is obtained after heat treatment at 1100 °C. Figure 5a demonstrates the pore size distributions measured for samples heat-treated at 1100 °C using the mercury intrusion method. A comparison with Figure 3 and Figure 5a reveals that the size of macropores becomes slightly small because of the shrinkage of network upon heating at 1100 °C, while keeping the sharp pore size distribution. A close look at Figure 5a indicates that pore size distributions at around 50 nm, which is independent of the PEO content, are observed, in addition to the pore size distribution in the micrometer range. Judging from the sharp peaks in XRD patterns for the sample heat-treated at 1100 °C, the appearance of relatively large mesopores are caused by the interstices among the particles

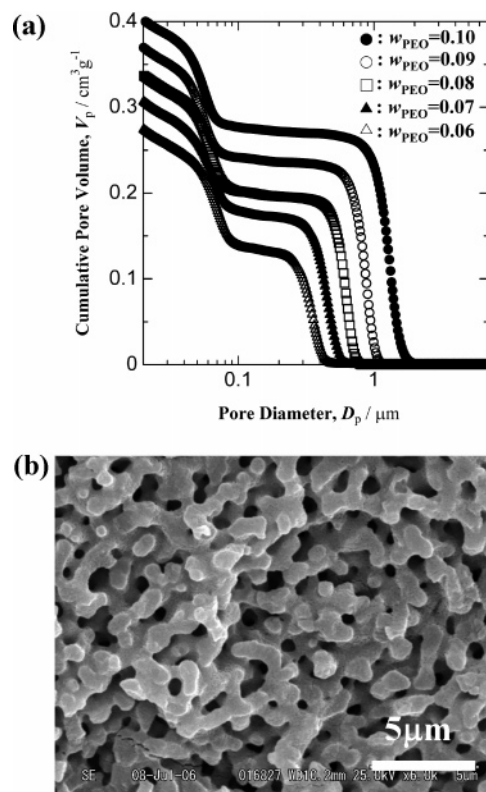


Figure 5. (a) Pore size distributions of samples heat-treated at 1100 °C. The measurements were carried out for the samples prepared from the HP system with $w_{\text{PEO}} = (\Delta) 0.06, (\blacktriangle) 0.07, (\square) 0.08, (\circ) 0.09$, and $(\bullet) 0.10$. (b) SEM image of the sample prepared from the HP system with $w_{\text{PEO}} = 0.08$ and then heat-treated at 1100 °C for 5 h.

grown during the heat treatment. A representative SEM image is shown for the sample prepared from the HP system with $w_{\text{PEO}} = 0.08$ and then heat-treated at 1100 °C. The bicontinuous macroporous structure is maintained without cracks, although the gel shrinks by about 50–60% after the heat treatment.

In contrast to the macroporous structure, micro–mesoporous structures are significantly altered by the heat treatment. Nitrogen adsorption–desorption isotherms of dried gel and those heat-treated at various temperatures are shown in Figure 6; the corresponding BJH pore size distributions are depicted in the inset. The measurements were carried out for the samples prepared from the HP system with $w_{\text{PEO}} = 0.09$. The dried gel and that heat-treated at 300 °C exhibit the isotherm of type IV according to the IUPAC classification, signifying the existence of mesopores. As revealed from the BJH pore size distribution, pores are distributed in the micro-to small mesopore region. The relatively sharp pore size distributions originate from the interstices among primary particles, implying the formation of a gel network with considerably fine mesh as a result of the homogeneous condensation of Al₂O₃ oligomers. By heat treatment at temperatures above 800 °C, the adsorption–desorption curves are changed into H2-type, indicating that the materials have the “ink bottle”-type mesopores expected to occur from the compaction of a globular or particulate gel structure. In the present case, the shape of mesopores may be associated with the sintering of nanoparticles comprising the skeleton. Heating at 800 °C, which leads to the precipitation of nanocrystalline γ -Al₂O₃ phase, increases the pore size

(20) Lippens, B. C. Ph.D. thesis. Delft University, Delft, The Netherlands, 1961.

(21) Gitzen, W. H. *Alumina as a Ceramic Material*; Wiley-American Ceramic Society: New York, 1970.

(22) Yoldas, B. E. *Am. Ceram. Soc. Bull.* **1975**, *54*, 286.

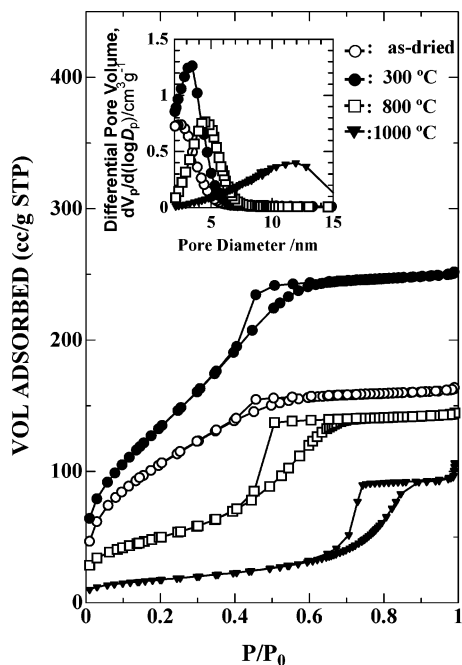


Figure 6. Nitrogen adsorption–desorption isotherms of samples prepared from the HP system with $w_{\text{PEO}} = 0.09$ and then heat-treated at varied temperature. Inset shows the corresponding pore size distribution curves calculated by the BJH method using the adsorption branches. Symbols \circ , \bullet , \square , and \blacktriangledown represent the data for the dried gel and those heat-treated at 300, 800, and 1000 °C, respectively.

Table 2. Structural Properties of Dried and Heat-Treated HP Samples Prepared with $w_{\text{PEO}} = 0.09$

heat-treated T (°C)	BET surface area (m^2/g)	median pore size (nm)
40 (as-dried)	396	2.6
300	512	3.5
500	362	4.0
700	250	4.2
800	182	4.5
900	117	6.1
1000	63	12

without disturbing a relatively sharp size distribution. In response to the precipitation of $\alpha\text{-Al}_2\text{O}_3$ during heat treatment at 1000 °C, the pore size becomes drastically large, and the pore size distribution becomes broad. The median pore size and BET surface area are summarized in Table 2. The dried gel exhibits the surface area of 396 m^2/g with a median pore size of about 2.6 nm. As the heat-treatment temperature is higher, the mesopores become larger in size because of the particle growth. On the other hand, the BET surface area increases to 511 m^2/g at 300 °C, and then decreases at elevated temperatures. The increase in surface area upon heating at 300 °C is mainly due to the removal of residual

organic species, although the particle growth and/or sintering during the heat treatment at higher temperatures reduces the surface area. Nevertheless, the surface area is still large ($\sim 182 \text{ m}^2/\text{g}$) when the heat-treatment temperature is raised to 800 °C, at which nanocrystalline $\gamma\text{-Al}_2\text{O}_3$ phase appears.

Conclusion

Macroporous Al_2O_3 with mesoporous skeletons has been prepared from the aqueous and ethanolic solution of aluminum chloride in the presence of propylene oxide and PEO. Polymerization-induced phase separation produces monolithic gels with well-defined macroporous bicontinuous structures. By adjusting the PEO content in the starting solution, the size of the macropores of dried gels can be controlled in the range of 400 nm to 1.8 μm . Even after heat treatment at 1100 °C, the macroporous structures are retained without spoiling the sharp pore size distribution. The dried gel possesses a BET surface area of 396 m^2/g and a median pore size of 2.6 nm, whereas heating at 300 °C increases the surface area and pore size to 511 m^2/g and 3.5 nm, respectively. The high surface area of 181 m^2/g is obtained even after heat treatment at 800 °C accompanied by the precipitation of nanocrystalline $\gamma\text{-Al}_2\text{O}_3$ from the amorphous phase. The synthetic technique as described here is very simple and reproducible, so it is expected that the resultant hierarchical macro–mesoporous Al_2O_3 monoliths find applications in fields such as separation media, catalyst supports, and so forth. Also, the present method is readily applicable to the fabrication of other hierarchical macro–mesoporous porous metal oxides, which will be reported elsewhere.

Acknowledgment. This study was supported by a Grant-in-Aid for Scientific Research (18360316) from the Ministry of Education, Culture, Sports, Science, and Technology (MEXT), Japan, and the Industrial Technology Research Grant Program (04A25023c) and the Grant for Practical Application of the University R&D Results under the Matching Fund Method from the New Energy and Industrial Technology Development Organization (NEDO), Japan. K.F. thanks The Mazda Foundation for a research grant.

CM063051P